Spectral Energy Distribution of Hyper-Luminous Infrared Galaxies

A. Ruiz (IFCA), F.J. Carrera (IFCA), F. Panessa (INAF-Rome), and G. Miniutti (Lab. APC-Paris)

Abstract The relationship between star formation and super-massive black hole growth is central to our understanding of galaxy formation and evolution. Hyper-Luminous Infrared Galaxies (HLIRGs) are unique laboratories to investigate the starburst-AGN connection, since they exhibit extreme star formation rates, and most of them show evidence of harbouring powerful AGN. We have performed an X-ray spectral study of a sample of HLIRGs observed with XMM-*Newton*, finding that the X-ray emission of most of these sources is dominated by AGN activity. To improve our estimate of the relative contribution of the AGN and starburst (SB) emission to its total bolometric output, we have built multi-wavelength (from radio to X-rays) spectral energy distributions (SED) for these HLIRGs, and we have fitted standard AGN and SB templates to these SEDs. We have found that most of our HLIRGs need an AGN template to model its SED, and this component dominates the bolometric output. We also have found that our sources classified as type 1 AGN are better modelled using a luminosity-dependent template. Extending the SED to the X-ray bands places better constraints on the relative contribution of the AGN and SB with respect to using only IR/sub-mm data.

1 Introduction

During the last decade strong evidences have been discovered supporting the hypothesis that Active Galactic Nuclei (AGN) and galaxy formation and evolution are closely related (1; 2; 3). These hints clearly suggest a connection between the growth of the central supermassive black holes through accretion and the growth of the spheroid of the galaxies through star formation.

The study of these two phenomena needs penetrating radiation like X-rays, mid-infrared (MIR), far-infrared (FIR) or sub-mm. Primary radiation of star formation

A. Ruiz
Instituto de Física de Cantabria (CSIC-UC), Santander 39005, Spain e-mail: ruizca@ifca.unican.es

and AGNs is often reprocessed by dust and reemitted in the MIR-FIR band (4; 5). Hence, IR and X-ray observations are essential to understand the phenomena of star formation and active galaxies.

Fortunately, at this time we have powerful tools to observe the Universe in both energy ranges, like *Chandra*, XMM-*Newton*, *Spitzer*, *Akari* or *Suzaku*. We can follow different strategies to obtain the IR/X-ray synergy on the study of the AGN-galaxy co-evolution, e.g. by multi-wavelength surveys like AEGIS, GOODS or COSMOS; or by targeted MIR observations of X-ray sources like X-ray absorbed QSO (6); or by targeted X-ray observations of strong IR-emitting objects like Ultraluminous Infrared Galaxies (ULIRGS, 7) or Hyperluminous Infrared Galaxies (HLIRGS, 8).

ULIRGs are a class of galaxies with IR luminosity $L_{IR} \geq 10^{12} L_{\odot}$, dominated by the emission in the infrared (IR) waveband. They are powered by SB and, in some cases (~ 50%), they harbour an AGN (9; 10; 11). Most of these objects are in interacting systems, i.e. ULIRGs are triggered by mergers of galaxies (12; 13).

HLIRGs present an IR luminosity $L_{IR} \geq 10^{13} L_{\odot}$. These are among the most luminous objects in the Universe. Assuming that the FIR emission above $50\mu m$ is originated in SB, their estimated star formation rates are > 1000 $M_{\odot} yr^{-1}$ (14). IR and optical observations support that most harbour an AGN (15; 16), although the main power source is still controversial. Only about a third are located in interacting systems, so we cannot just classify them as the high luminosity tail of ULIRGs (17). They could be very young galaxies experiencing their major episode of star formation (14), or may be a completely new class of objects, e.g. a transient IR-luminous phase in quasar evolution (16).

HLIRGs present extreme star formation and a high AGN fraction, so they are excellent laboratories to investigate the connection between ultimate star formation and BH growth.

Here we present the results of an X-ray study of a sample of HLIRGs observed with XMM-*Newton* (Sect. 2) and the modelling of the multi-wavelength spectral energy distribution (SED) of these sources, using templates of standard SB galaxies and AGNs (Sect. 3).

2 XMM-*Newton* study of HLIRGs

The Sample

We have done the first systematic study of HLIRGs in the X-ray band (8). We chose those HLIRGs from the Rowan-Robinson sample (14) with public data available in the XMM-*Newton* Science Archive as of December 2004, and we added our own XMM-*Newton* AO-5 data. We limited this sample to sources with redshift less than ~ 2 to avoid strong biasing towards high redshift quasars. We also rejected one source, IRAS 13279+3401, because recent data in the optical and the MIR reveals that the redshift presented in the literature was too high, misclassifying it as HLIRG.

We have thirteen objects in our final sample (see Table 1), all of them with SED fitting in the MIR/FIR band (14; 15; 16).

In accord with their optical spectra (derived from the literature), two sources are classified as SB galaxies and twelve sources present AGN characteristics. Eight of them are classified as ‘type 1’, and four of them as ‘type 2’. All ‘type 2’ and one NL-SB galaxy are Compton-Thick (CT) candidates.

Results

We can summarize the results of our X-ray study as follows. Ten out of 13 objects were detected by XMM-*Newton*. All of them present an AGN dominated X-ray spectra. The IR luminosity of most sources is consistent with an AGN origin, but it is systematically over that expected for a local QSO (18; 19) of the same X-ray luminosity (see Fig. 1).

We detected soft thermal emission associated with a SB in just one source. There are four more sources with a thermal component, but their luminosities are consistent with the typical type 1 AGN soft excess.

In addition, our analysis of the CT candidates supports the heavily absorbed nature of these objects.

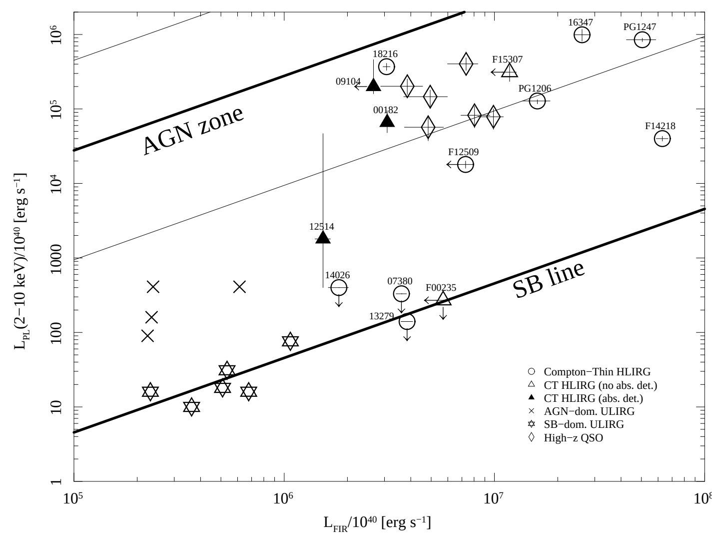

Fig. 1 2-10 keV X-ray luminosity of the power law component versus FIR luminosity (40-500 μm). Filled symbols represent sources where we have detected X-ray absorption. “AGN-zone” indicates the X-ray luminosity expected for an AGN of a given FIR luminosity (18; 19). The “SB-line” indicates the X-ray luminosity expected for a SB of a given FIR luminosity (20; 21).

3 Spectral Energy Distributions

We have seen that most HLIRGs in our sample present a systematic IR excess with respect to the mean luminosity expected to AGNs. This could be due to X-ray obscuration, SB emission or may be due to an intrinsic difference between the SED of AGN in HLIRGs and the SED of local QSO. Our aim was also to check the presence of AGN and/or SB emission in these sources and estimate the contribution of these components to the total output.

To solve these questions, we have built and modelled the SED of every source in our sample, from radio to X-rays. To this end, we have done an intensive search in the literature and in several astronomical databases.

We fitted the SED of our HLIRGs with a simple model based on templates. This model comprise two added components, one associated to the AGN emission and the other associated to the SB emission. The normalization of each component are the only free parameters in our model.

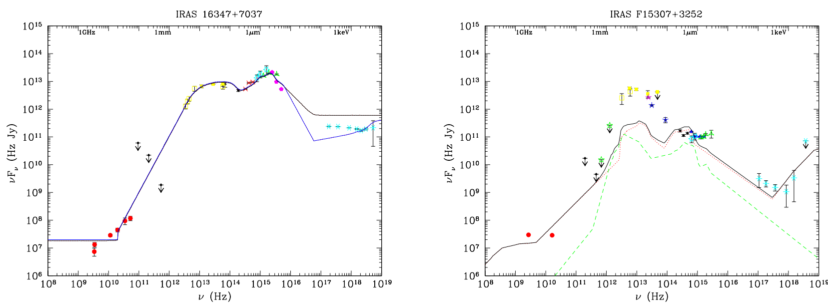

(a) IRAS 16347+7037 (b) IRAS F15307+3252

Fig. 2 SEDs of two HLIRGs, optically classified as type 1 AGN (left) and type 2 AGN (right). Green slashed lines are the SB templates, red dotted lines are the AGN templates, black solid lines are the total template (AGN+SB). Blue lines are luminosity dependent type 1 AGN templates

Starburst and AGN templates

As templates we employed the observed SED of standard SB galaxies and AGNs. On one hand, as SB templates we used four objects. They present different levels of obscuration, width and peak wavelength.

On the other hand, we used six AGN templates: the mean SED of radio quiet and radio loud local QSO (18; 22), and the SED of four type 2 sources. These four sources have column densities varying from 10^{22} cm^{-2} (Compton thin objects) to greater than 10^{25} cm^{-2} (Compton thick objects). They were selected from a sample of Seyfert 2 galaxies with minimal SB contribution (23).

We have also used a luminosity dependent QSO SED as template for those sources classified as type 1 AGN (24).

Results

Fig. 2 shows some examples of the SED of our HLIRGs and their best fit models. These fits could be improved using more complex and detailed models but we could get some interesting results.

Table 1 summarized the results of this analysis. The SEDs are roughly well fitted with this simple model and their best fits are consistent with the optical classification of most sources (11 out of 13).

We could fit five HLIRGs with pure AGN models, and four with composite models (AGN and SB templates are needed). We also fit four sources with just SB templates. However, only 2 out of 5 sources classified as CT candidates need a CT template in their models. We found that 9 out of 13 sources need an AGN component. The bolometric output of these objects is clearly dominated by the AGN emission.

We could see that the mean QSO SED overpredicts the X-ray flux of our type 1 sources, as we found in the previous X-ray analysis. We fitted these objects with a luminosity dependent SED template, finding a better prediction of its X-ray emission (e.g. Fig. 2(a)).

Table 1 Best fit models for the HLIRG's SEDs

Source	Type	Best Fit model[a]		$\log L_{BOL}$[b]	AGN / SB[c]	CT[d]
IRAS 00182-7112	QSO 2	-	SB1	46.1	0 / 1	Y
IRAS F00235+1024	NL-SB	-	SB4	45.6	0 / 1	Y
IRAS 07380-2342	SB	-	SB1	46.2	0 / 1	N
IRAS 09104+4109	QSO 2	AGN3	SB1	46.9	0.6 / 0.4	Y
PG 1206+459	QSO	AGN1	-	48.4	1 / 0	N
PG 1247+267	QSO	AGN1	-	49.2	1 / 0	N
IRAS F12509+3122	QSO	AGN1	-	47.4	1 / 0	N
IRAS 12514+1027	Sy2	AGN5	SB2	47.2	0.5 / 0.5	Y
IRAS 14026+4341	QSO	-	SB4	46.8	0 / 1	N
IRAS F14218+3845	QSO	AGN1	-	47.0	1 / 0	N
IRAS F15307+3252	QSO 2	AGN5	SB4	47.0	0.8 / 0.2	Y
IRAS 16347+7037	QSO	AGN1	-	48.9	1 / 0	N
IRAS 18216+6418	QSO	AGN1	SB1	47.5	0.7 / 0.3	N

[a] Templates: AGN1,AGN2: radio quiet/loud mean QSO SED; AGN3: NGC 5506; AGN4: NGC 4507; AGN5: Mnk 3; AGN6: NGC 3393. SB1: NGC 1482; SB2: NGC 4102; SB3: NGC 5253; SB4: NGC 7714. [b] Bolometric luminosity in CGS units. [c] Fraction of the bolometric luminosity originated in AGN and/or SB. [d] Compton Thick candidates.

4 Conclusions

We have done a systematic study of a sample of 13 HLIRGs. We first analysed the XMM-*Newton* spectra of this sources and then we built and modelled their multi-wavelength SED (from radio to X-rays). Our results can summarized as follow:

1. Ten out of 13 sources were detected in X-rays, showing AGN-dominated spectra.
2. These AGN-dominated HLIRGs are less luminous in X-rays than the estimate using the mean local QSO SED.
3. Nine out of 10 X-ray detected HLIRGs needed an AGN component in its SED, and this component dominates the bolometric luminosity.
4. The SED best fits are consistent with the optical classification.
5. The SED of our HLIRGs classified as type 1 AGN are consistent with a luminosity dependent quasar SED.
6. X-ray data are mandatory to get an accurate estimation of the relative contribution of AGN an SB to the total output.

References

[1] J. Kormendy et al., *AIP Conference Series*, vol. 586, pp. 363–+
[2] R.J. McLure, J.S. Dunlop, MNRAS **331**, 795 (2002).
[3] J.D. Silverman et al., ApJ **624**, 630 (2005).
[4] A.C. Fabian, K. Iwasawa, MNRAS **303**, L34 (1999)
[5] Y. Ueda et al., ApJ **598**, 886 (2003).
[6] J.A. Stevens et al., MNRAS **360**, 610 (2005).
[7] A. Franceschini et al., MNRAS **343**, 1181 (2003).
[8] A. Ruiz, F.J. Carrera, F. Panessa, A&A **471**, 775 (2007).
[9] D. Farrah et al., ApJ **626**, 70 (2005).
[10] S.H. Teng et al., ApJ **633**, 664 (2005).
[11] E. Nardini et al., MNRAS **385**, L130 (2008).
[12] D. Farrah et al., MNRAS **326**, 1333 (2001).
[13] S. Veilleux, D.C. Kim, D.B. Sanders, ApJs **143**, 315 (2002).
[14] M. Rowan-Robinson, MNRAS **316**, 885 (2000)
[15] A. Verma et al., MNRAS **335**, 574 (2002).
[16] D. Farrah et al., MNRAS **335**, 1163 (2002).
[17] D. Farrah et al., MNRAS **329**, 605 (2002).
[18] M. Elvis et al., ApJs **95**, 1 (1994).
[19] G. Risaliti et al., *A Panchromatic View of AGN* (ASSL Vol. 308, 2004), p. 187
[20] M. Persic et al., A&A **419**, 849 (2004).
[21] R.C. Kennicutt, ApJ **498**, 541 (1998).
[22] G.T. Richards et al., ApJs **166**, 470 (2006).
[23] S. Bianchi et al., A&A **448**, 499 (2006).
[24] P.F. Hopkins et al., ApJ **654**, 731 (2007).